

Published in final edited form as:

Transgenic Res. 2014 August ; 23(4): 631–641. doi:10.1007/s11248-014-9799-7.

Generation of mice encoding a conditional null allele of *Gcm2*

Ziqiang Yuan¹, Evan E. Opas², Chakravarthy Vrikshajanani¹, Steven K. Libutti¹, and Michael A. Levine²

¹Department of Surgery, Albert Einstein College of Medicine of Yeshiva University, Bronx, NY 10461, USA

²Division of Endocrinology and Diabetes, The Children's Hospital of Philadelphia and Department of Pediatrics, Perelman School of Medicine of the University of Pennsylvania, Philadelphia, PA 19104, USA

Abstract

Glial cells missing homolog 2 (GCM2) is a transcription factor that is expressed predominately in the pharyngeal pouches and, at later stages, in the developing and mature parathyroid glands. In humans, loss of GCM2 function, either through recessive apomorphic mutations or dominant inhibitor mutations in the human *GCM2* gene, leads to isolated hypoparathyroidism. In mice, homozygous disruption of *Gcm2* by conventional gene targeting results in parathyroid aplasia and hypoparathyroidism. In this study, we report the generation and functional characterization of mice encoding a conditional null allele of *Gcm2*. We demonstrate the functional integrity of the conditional *Gcm2* allele and report successful *in vivo* deletion of exon 2 using Cre recombinase. The mice with conditional deletion of *Gcm2* displayed phenotypes similar to those previously described for a conventional *Gcm2* knockout, including perinatal lethality, hypocalcemia, low or undetectable serum levels of parathyroid hormone (PTH), and absent parathyroid glands. The production of a conditional mutant allele for *Gcm2* represents a valuable resource for the study of the temporal- and spatial-specific roles for *Gcm2*, and for understanding the postnatal activities of GCM2 protein.

Keywords

Gcm2; parathyroid hormone; parathyroid gland; knockout mice

Introduction

Glial cell missing homolog 2 (GCM2) is a homolog of the *gcm/glide* gene that was originally identified in *Drosophila melanogaster*. (Hosoya et al. 1995; Wegner and Riethmacher 2001) In the fly, *gcm* and the related *gcm2* are specifically and transiently expressed in the central nervous system where they act as binary switches to promote glial cell fate while simultaneously inhibiting the neuronal fate. These two genes function

Corresponding Author: Michael A. Levine, MD, Division of Endocrinology and Diabetes, The Children's Hospital of Philadelphia, 34th and Civic Center Blvd, Philadelphia, PA 19104, Tel 215.590.3618, Fax 215.590.3053, levinem@chop.edu.

Disclosure: All authors have nothing to disclose

redundantly and are required for the formation of a subset of glial cells. (Akiyama et al. 1996; Chotard et al. 2005) By contrast, vertebrate GCM2 is expressed predominately in the pharyngeal pouches and, at later stages, in the developing and mature parathyroid glands of tetrapods and in the internal gill buds in fish.(Okabe and Graham 2004; Zajac and Danks 2008) In addition to *Gcm2*, a second vertebrate *gcm* homolog, *Gcm1*, has been identified that is expressed in villous cytotrophoblast cells of the placental and is essential for both syncytiotrophoblast differentiation and formation of chorionic villi. (Hashemolhosseini and Wegner 2004). All members of the GCM family encode nuclear transcription factors that contain a unique DNA binding domain (*i.e.* the GCM motif) in the amino terminus, one or two transactivation domains, and several potential PEST sequences that are typical of proteins displaying a rapid turnover. (Kim et al. 1998; Jones et al. 1995; Hosoya et al. 1995; Altshuller et al. 1996; Kammerer et al. 1999; Hashemolhosseini and Wegner 2004) Sequence homology between members of the GCM family is greatest within the GCM motif. (Cohen et al. 2003; Cohen et al. 2002; Schreiber et al. 1998)

Conventional deletion of the *Gcm2* gene in transgenic mice leads to parathyroid aplasia and hypoparathyroidism, a metabolic condition characterized by hypocalcemia and hyperphosphatemia due to absence of parathyroid hormone (PTH).(Gunther et al. 2000; Kamitani-Kawamoto et al. 2011; Hitoshi et al. 2011) In humans, loss of GCM2 activity, through either recessive amorphic (Ding et al. 2001; Maret et al. 2008; Sticht and Hashemolhosseini 2006; Baumber et al. 2005; Thomee et al. 2005; Doyle et al. 2012) or dominant inhibitor(Mannstadt et al. 2008; Mirczuk et al. 2010; Canaff et al. 2009) mutations in *GCM2*, is an important cause of idiopathic hypoparathyroidism. Current knowledge about the role of GCM2 in parathyroid homeostasis has come from developmental analyses in mice (Gordon et al. 2001; Liu et al. 2007; Grigorieva et al. 2010), which indicate that GCM2 is not necessary for pouch patterning or establishment of the parathyroid domain (*i.e.* induction of parathyroid cell precursors), but instead is required for differentiation and subsequent survival of parathyroid cells during embryogenesis. However, GCM2's role(s) in controlling parathyroid cell proliferation, survival or function during late embryological development and in the postnatal parathyroid gland is still unknown. In addition, recent studies that demonstrate transient expression of *Gcm2* in regions of the central nervous system during early development (Hitoshi et al. 2011) suggest that GCM2 may play a wider role that is cell- and context-specific. Hence, a key challenge will be to dissect out the function of GCM2 within various cells at different times during development and in mature tissues. This obviously cannot be accomplished by a simple constitutive knockout approach as performed previously. (Gunther et al. 2000; Hitoshi et al. 2011) These studies would be greatly facilitated or made possible, however, using mice harboring *Gcm2* conditional null alleles. We report here the generation and characterization of such mice using DNA homologous recombination in embryonic stem (ES) cells and the Cre-loxP and FLP-FRT technologies.

MATERIALS AND METHODS

Generation of a *Gcm2*-floxed Allele

The C57BL/6 mouse chromosome 13 sequence (n.t.# 41,112,399–41,121,157) was retrieved from the Ensembl database (www.ensembl.org) and used as a reference in this project. The RP23-2H11 bacterial artificial chromosome (BAC) was used to generate the homologous arms and the conditional knockout (CKO) region for the gene targeting vector, as well as the probes for screening targeted events by restriction endonuclease analysis (Figure 1). The 5' homologous arm (4.2 kb), 3' homologous arm (4.0 kb) and CKO region that includes exon 2 (252 bp) were generated by PCR. The fragments were cloned in the LoxFtNwCD vector (Taconic Laboratory) or pCR4.0 for sequencing. The final targeting construct was obtained by standard molecular cloning (Figure 1B). Briefly, the CKO region was cloned in *BsiWI*/*SaII* sites, upstream from the FRT site in the vector, using PCR (primers used: Cl_GCMB_E2F, 5'-actgcgtacgCCTATTCTGTTTGCCATCTTTTCCC-3' and Cl_GCMB_E2R, 5'-actggtcgacGGAAGGTAGAGGGACACCAGCTAGG-3') (Figure 1). The 5'-arm was cloned into LoxFtNwCD at *NotI*/*AvrII* sites, upstream from loxP site (Primers: Cl_GCMB_5F, 5'-actggcgccgcCCTTCTGTCTCTTTCTGTCTCAGTCTCC-3' and Cl_GCMB_5R: 5'-actgctaggGGAAAAGATGGCAAACAGAATAGGAC-3'). The 3' arm was cloned in LoxFtNwCD in *AscI*/*NruI* sites (primers: Cl_GCMB_3F: 5'-actggcgccgcCTCTGTTCCTAGCTGGTGTCCCTCTACC-3' and Cl_GCMB_3R: 5'-actgtcgcaGGCAAGGCTAGTTGACTTGTGTCTAA-3'). Aside from the homologous arms, the final vector also contains *loxP* sequences flanking the region targeted for deletion (433 bp), FRT sequences flanking the *Neo^r* expression cassette (for positive selection of the ES cells), and a diphtheria toxin (DTA) expression cassette (for negative selection of the ES cells). The final vector was confirmed by both restriction digestion and end sequencing analysis. The 5' and 3' external probes were generated by PCR and were tested by genomic Southern blot analysis for screening of the ES cells. The positions of the probes used for Southern blot analysis are shown in Figure 1C. *NotI* was used to linearize the final vector prior to electroporation into B6 embryonic stem (ES) cells (Taconic Laboratory). We transfected properly targeted clones with FLP recombinase, and genotyped replicate colonies that had lost resistance to G418 by PCR. In order to confirm that the *loxP* sites were functional in the floxed *Gcm2^{tm1Mal2}* (i.e. *Gcm2^{E2fl}*) alleles, we electroporated *Neo^r*-deleted clones with *Cre* recombinase, isolated genomic DNA, and analyzed the *Gcm2* gene for proper recombination and loss of exon 2 (i.e. *Gcm2^{E2}*). Two ES clones containing properly recombined *Gcm2^{tm1Mal2}* alleles were injected blastocysts from B6(Cg)-*Tyr^{c-2J}*/J albino mice (Jackson Laboratory stock #000058) to generate chimeric mice. The resultant chimeras were mated with C57BL/6NTac females and F1 black offspring were genotyped by PCR and Southern blot analyses. Mice carrying the conditional allele were homozygosed by mating *Gcm2^{E2fl/+}* animals, producing *Gcm2^{E2fl/E2fl}* mice. Both male and female heterozygous and homozygous animals were subjected to metabolic study. We bred female mice that were heterozygous for the conditional allele with 129S/Sv-*Tg(Prm-cre)58Og/J* males (Jackson Laboratory stock #003328) to generate mice that were heterozygous for *Gcm2* lacking exon 2 (i.e. *Gcm2^{E2}*). B6;129Sv-*Gcm2^{tm1.1Mal2}* mice have generalized inactivation of *Gcm2* alleles. Mice were maintained on a 129SvE;C57BL/6NTac hybrid genetic background as high lethality had been previously reported for constitutive *Gcm2*

knockout mice on a non-hybrid background.(Gunther et al. 2000) The mice produced for this project were fed Pico Lab Rodent diet 20–5053 while in holding cages and Pico Lab Mouse diet 20–5058 while in the breeding cages. All animal experiments were conducted according to protocols approved by The Children’s Hospital of Philadelphia and Albert Einstein College of Medicine.

Genotyping

Genotypes were determined by Southern blot both with 5’ and 3’ external probes (Figure 1, panels C and D). For initial PCR screening of floxed alleles, we used forward primer 5’-GGTTTCCAAATGTGTCTAGTTTCATAGCCT-3’ and reverse primer 5’-GGAAGAACTACTAAACCCACCAGACTGC-3’ (PCR primers shown in Figure 1, panel C, with the forward primer annealing in the *Neo^r* gene approximately 100 bp from 3’ end and reverse primer annealing 120 bp downstream of the 3’ homologous arm), with expected size of the amplified product approximately 4.1 kb (not shown). Diagnostic PCR for *in vivo* Cre recombinase-induced deletion of the CKO region used forward primer 5’-GATGCAGCTGGAGATTGACATTGTATAC-3’ and reverse primer 5’-GGCAAGGAACCAGCTCCAAAG-3 (Figure 1, panels E-G).

Biochemical Analyses

Whole blood and serum were collected using methods described previously (Germain-Lee et al. 2005). Total calcium and phosphate were measured using colorimetric assays (QuantiChrome Calcium Assay Kit DICA-500 and QuantiChrome Phosphate Assay Kit DIPA-500) from BioAssay Systems, Hayward, CA, USA. PTH was measured with an ELISA for rodent PTH 1–34 that has a detection limit of 1.6 pg/mL (Immutopics, San Clemente, CA, USA). Levels of intact FGF23 were measured using a mouse FGF23 ELISA kit that detects intact hormone (Kainos Laboratories, Inc., Tokyo, Japan). We measured serum 1,25(OH)₂D by ELISA using a kit from Immunodiagnostic Systems (Fountainhead, AZ, USA).

Histology

Mice were euthanized at postnatal 30 days, and tracheal blocks and other organs were dissected, formalin-fixed and embedded in paraffin and 5- μ m sections were prepared for subsequent analyses. To determine parathyroid gland size, appropriate tissue sections were digitalized and maximal parathyroid cross-sectional area was measured by computerized pixel counting. For immunofluorescence (IF) staining, paraffin sections were incubated with primary antibodies to calcium-sensing receptor (CASR) (1:50, rabbit polyclonal antiserum #33821, Santa Cruz Biotechnology), PTH (1:200, mouse monoclonal antiserum AB63993, Abcam), GCM1 (1:50, rabbit polyclonal antiserum 98811, Santa Cruz Biotechnology) or GCM2 (1:50, goat polyclonal antiserum 79495, Santa Cruz Biotechnology) at 4° C overnight. Antibody binding was detected by incubation with appropriate secondary antibodies (anti-mouse Alexa Fluor 647, anti-rabbit Alexa Fluor 488, and anti-goat Alexa Fluor 488, Invitrogen) at 1:200 dilution for 45 minutes in the dark. Finally, the sections were stained with 4’6-diamidino-2-phenylindole (DAPI) (Vector Laboratories, Burlingame, CA) and imaged by fluorescence microscopy.

Statistical analyses

Data were analyzed using GraphPad InStat v3.06 for Windows (GraphPad Software). Means were compared using Student's t-test. All results are expressed as the mean \pm SD. Statistical significance was accepted at $P < 0.05$.

Results

Generation of the Conditional Allele of *Gcm2*

The mouse *Gcm2* gene is organized into five exons, with exon 1 containing the start codon and the first 30 amino acids of the protein, exon 2 containing the entire GCM motif, and exons 3–5 encoding the C-terminal two thirds of the protein (Figure 1). Two groups have developed *Gcm2* knockout mice with constitutive deletions. Günther *et al.* used a targeting vector that replaced exons 2–5 of *Gcm2* (>5 kb) with the gene encoding neomycin resistance (*Neo^r*) (*Gcm2^{tm1Kry}*) to create conventional *Gcm2* knockout mice (*129S7-Gcm2^{tm1Kry}*), (Gunther et al. 2000), whereas Hitoshi *et al.* replaced exons 2–5 with the *LacZ* gene. (Hitoshi et al. 2011) To generate a conditional allele for *Gcm2*, we inserted two *loxP* sites in the same orientation to flox exon 2 (*Gcm2^{E2fl}*), such that *Cre*-mediated recombination would result in excision of exon 2 (*Gcm2^{E2}*) (Figure 1E). Splicing of E1 into E3 was predicted based on the gene sequence to create a frameshift rapidly followed by a stop codon, and thus to result in production of a short peptide lacking the two main functional domains of *Gcm2*. Hence, the *Gcm2^{E2}* allele (*Gcm2^{tm1Mal2}*) would be a null allele of *Gcm2*.

The *Gcm2* targeting construct was electroporated into ES cells and 4 clones (C5, H3, H11, E8) were positively identified by PCR and were expanded. Two clones, H11 and E8, were confirmed by Southern analysis (Figure 1D) with all 3 probes to contain the properly targeted *Gcm2^{E2fl-Neo}* allele.

We transfected clones E8 and H11 with FLP recombinase and selected 96 colonies from each clone for replicate testing for G418 sensitivity. A number of G418-sensitive clones were selected and analyzed by PCR, which confirmed deletion of the *Neo^r* gene and the presence of 5' *loxP* sites (Figure 1F). To assure that the *loxP* sites were functional in the *Gcm2^{E2fl}* alleles, we electroporated *Neo^r*-deleted clones with *Cre recombinase*. These cells were grown for several days and then batch-harvested for isolation of genomic DNA, and PCR confirmed the excision of E2 (data not shown). We used both clones E8 and H11 to generate mouse male chimeras. These mice transmitted the *Gcm2^{tm1Mal2}* floxed allele to their progeny. Both mouse lines were maintained and one is described here.

Recombination of the floxed *Gcm2^{tm1Mal2}* Allele *in Vivo*

The floxed *Gcm2^{E2fl}* was converted into the inactive *Gcm2^{E2}* by breeding homozygous *Gcm2^{tm1Mal2}* females with *129S/Sv-Tg(Prm-cre) 580g/J* males (Jackson Labs stock# 003328) that are homozygous for the *Protamine-Cre (Prm-cre)* trans-gene, which is expressed exclusively in the male germ line. (O'Gorman and Wahl 1997; O'Gorman et al. 1997) The cloned "CKO" fragment is 347 bp (95 bp longer than E2), and FLP treatment left an additional piece (frrt + linker), which made the actual deleted piece 433 bp long. Subsequent matings of *Gcm2^{E2fl/+};Prm-cre* male progeny with wildtype females yielded

Gcm2^{E2/+} progeny. Those mice that did not carry the *Prm-cre* transgene were intercrossed for analysis (see below). All mice were genotyped by PCR using strategies designed to readily identify the *Gcm2*, *Gcm2*^{E2fl}, and *Gcm2*^{E2} alleles (Figure 1G).

Phenotype of the Cre-recombined *Gcm2* Mice

Gcm2^{E2fl/+}, *Gcm2*^{E2fl/E2fl}, and *Gcm2*^{+/+} mice were viable and obtained at the expected Mendelian ratios. Serum levels of calcium, phosphate and PTH were normal in all genotypes (data not shown). Subsequent matings of *Gcm2*^{E2/+} mice generated *Gcm2*^{E2/E2} progeny that were viable but with an apparent 30% lethality, similar to that previously reported in the *B6;129S7-Gcm2^{tm1Kry}* mice. (Liu et al. 2010; Gunther et al. 2000) Wild type, floxed and knockout mice were of similar weight and length from weaning through 20 months; data at six months of age are shown in Table 1. By contrast, biochemical analyses demonstrated significant differences between the knockout mice and the floxed and wild type mice (Table 1): serum calcium was lower and serum phosphate was greater in knockout mice than in wild type or floxed mice and serum levels of PTH were undetectable in sixteen and extremely low in seven of twenty-three *Gcm2*^{E2/E2} mice. Moreover, serum 1,25(OH)₂D levels were lower (120.3 ± 33.9 pmol/L) in knockout mice compared to those in wildtype mice (160.6 ± 31.8 pmol/L). And finally, serum levels of intact FGF23 were significantly (*P* < 0.05) lower in knockout mice (63.4 ± 35 pg/mL) than in wildtype mice (137.8 ± 35 pg/mL).

Analysis of the thyroïdal area indicated that knockout mice lacked parathyroid tissue, whereas floxed mice had parathyroid tissue of normal size (Figure 2A). Knockout mice also showed no expression of PTH, CASR (Figure 2B) and GCM2 (GCM2) in the neck. The knockout mice showed normal development of other major organs, including, thymus, brain, lung, heart, liver, pancreas, testis, and ovary (data not shown). Wild type and knockout mice showed equivalent expression of CASR (Figure 3) and GCM1 (Figure 4) in the thymus and kidney.

Discussion

We have generated a conditional *Gcm2* allele that is fully active, and shown that generalized deletion of exon 2 is associated with parathyroid aplasia and hypoparathyroidism. Our knockout model differs from previous mouse models of constitutive ablation of *Gcm2* in which the approach led to insertion of either the *Neor* (Gunther et al. 2000) or *lacZ* (Hitoshi et al. 2011) genes into the *Gcm2* locus.

Serum levels of PTH were initially reported to be normal in *B6.129S7-Gcm2^{tm1Kry} Gcm2* knockout mice, which led to the proposal that thymic epithelial cells that co-expressed GCM1 and PTH represented an auxiliary source of circulating PTH. (Gunther et al. 2000) No information about mineral metabolism was reported in a second constitutive *Gcm2* knockout model. (Hitoshi et al. 2011) Subsequent reports demonstrated low or undetectable levels of serum PTH in the *B6.129S7-Gcm2^{tm1Kry}* mouse line, however (Simmonds et al. 2010; Liu et al. 2010), similar to the data that we present here. In the present work we identified immunoreactive PTH within a few thymus cells in wild type and homozygous knockout mice, consistent with the proposal that expression of PTH in medullary thymic

epithelial cells provides a source of self-antigen for negative selection. (Liu et al. 2010) Recent work has excluded the thymus as a source of circulating PTH in humans and mice (Maret et al. 2004; Liu et al. 2010). Similarly, the minimal expression of PTH in kidney cells that we identified, as well as previous demonstrations of PTH in the hypothalamus (Nutley et al. 1995; Fraser et al. 1990; Gunther et al. 2000), are unlikely to be physiologically significant. Although we have no certain explanation for the presence of low circulating levels of PTH in some of our knockout mice, this is similar to what we and others have described in humans with hypoparathyroidism due to inactivating *GCM2* mutations (Canaff et al. 2009; Mannstadt et al. 2008). As one proposed role for *GCM2* is to ensure parathyroid cell survival after initial specification of the parathyroid domain within the pouch endoderm (Liu et al. 2007), it is possible that small numbers of parathyroid cells can escape apoptosis in the absence of *GCM2* and secrete measurable if physiologically insignificant amounts of PTH.

Finally, we found that serum levels of FGF23 were not elevated in our homozygous knockout *Gcm2* mice, which lack parathyroid tissue, similar to that described in mice in which the *Pth* gene had been deleted (Yuan et al. 2013; Quinn et al. 2013). These observations are consistent with emerging evidence for a complex regulatory mechanism for FGF23 secretion that involves PTH (Silver and Naveh-Manly 2012) as well as serum concentrations of calcium and phosphorus to ensure a normal calcium \times phosphorus product (Quinn et al. 2013). By contrast, previous studies of patients with chronic (Gupta et al. 2004) or acute and transient hypoparathyroidism (Yamashita et al. 2007) had shown that levels of serum FGF23 were increased, and were correlated with hyperphosphatemia. But in these cases the patients were also receiving calcitriol or 1 α -hydroxyvitamin D, which would increase FGF23 (Collins et al. 2005; Gupta et al. 2004).

In conclusion, the *Gcm2* conditional null allele that we have generated will constitute a very valuable tool to block expression of *Gcm2* conditionally, in specific cell types and times *in vivo*. It will allow or greatly facilitate studies on the roles of *Gcm2* in multiple developmental, physiological, and even pathological processes in the mouse from embryogenesis onto adulthood, and will further elucidate the regulation of parathyroid development and extracellular calcium homeostasis.

Acknowledgments

This work was supported, in part, by NIDDK R01DK079970 (MAL), the Cleveland Clinic Lerner Research Institute, the CHOP Research Institute, the Albert Einstein College of Medicine and a generous gift from Linda and Earle Altman (SKL). We acknowledge the generous help and guidance of Dr. Alexander Gorodinsky, Taconic Laboratory.

References

- Akiyama Y, Hosoya T, Poole AM, Hotta Y. The gcm-motif: a novel DNA-binding motif conserved in *Drosophila* and mammals. *Proc Natl Acad Sci U S A*. 1996; 93(25):14912–14916. [PubMed: 8962155]
- Altshuller Y, Copeland NG, Gilbert DJ, Jenkins NA, Frohman MA. *Gcm1*, a mammalian homolog of *Drosophila* glial cells missing. *FEBS Lett*. 1996; 393(2–3):201–204. [PubMed: 8814290]

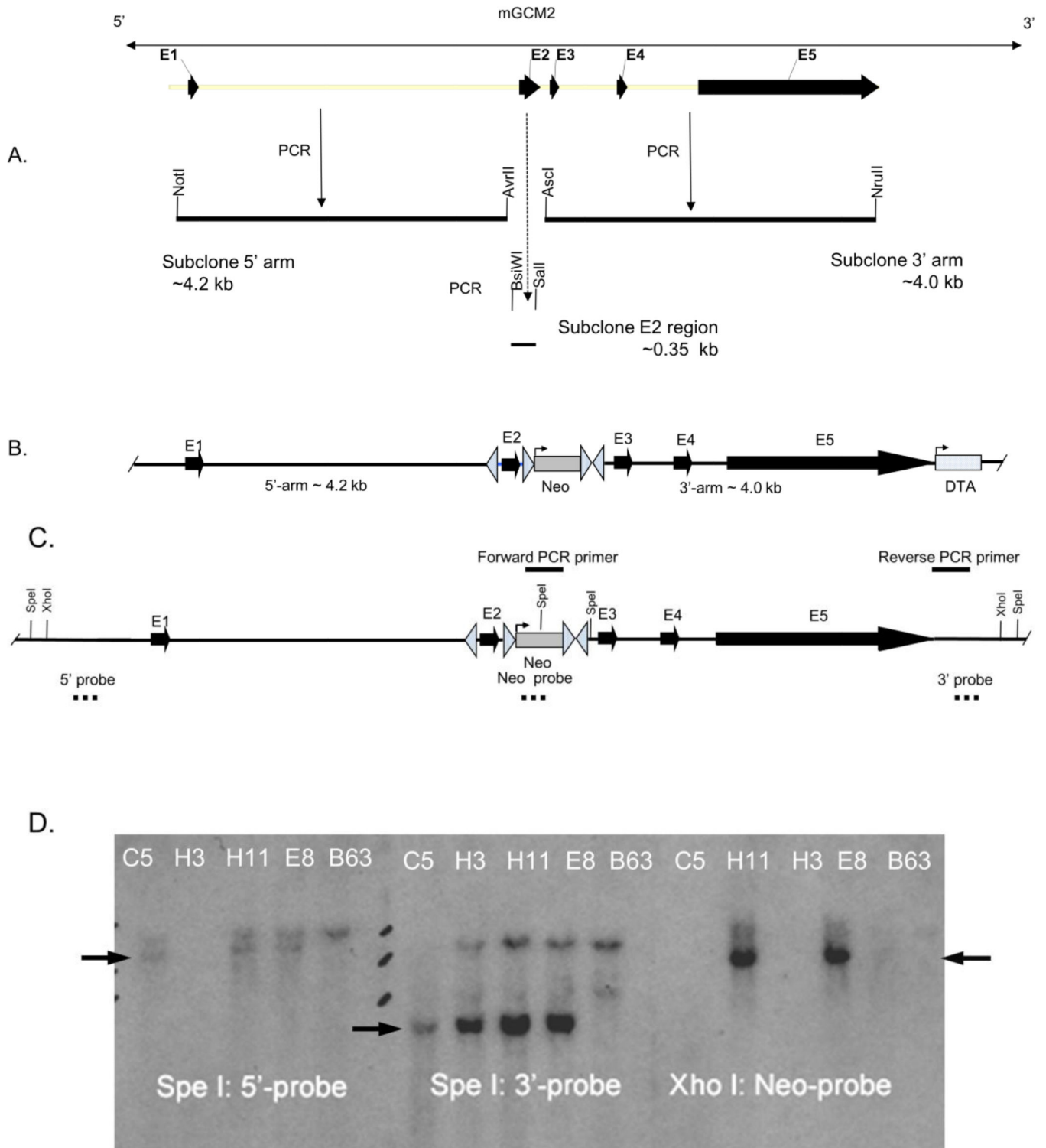
- Baumber L, Tufarelli C, Patel S, King P, Johnson CA, Maher ER, Trembath RC. Identification of a novel mutation disrupting the DNA binding activity of GCM2 in autosomal recessive familial isolated hypoparathyroidism. *J Med Genet.* 2005; 42(5):443–448. [PubMed: 15863676]
- Canaff L, Zhou X, Mosesova I, Cole DE, Hendy GN. Glial cells missing-2 (GCM2) transactivates the calcium-sensing receptor gene: effect of a dominant-negative GCM2 mutant associated with autosomal dominant hypoparathyroidism. *Hum Mutat.* 2009; 30(1):85–92. [PubMed: 18712808]
- Chotard C, Leung W, Salecker I. Glial cells missing and gcm2 cell autonomously regulate both glial and neuronal development in the visual system of *Drosophila*. *Neuron.* 2005; 48(2):237–251. [PubMed: 16242405]
- Cohen SX, Moulin M, Hashemolhosseini S, Kilian K, Wegner M, Muller CW. Structure of the GCM domain-DNA complex: a DNA-binding domain with a novel fold and mode of target site recognition. *EMBO J.* 2003; 22(8):1835–1845. [PubMed: 12682016]
- Cohen SX, Moulin M, Schilling O, Meyer-Klaucke W, Schreiber J, Wegner M, Muller CW. The GCM domain is a Zn-coordinating DNA-binding domain. *FEBS Lett.* 2002; 528(1–3):95–100. [PubMed: 12297286]
- Collins MT, Lindsay JR, Jain A, Kelly MH, Cutler CM, Weinstein LS, Liu J, Fedarko NS, Winer KK. Fibroblast growth factor-23 is regulated by 1 α ,25-dihydroxyvitamin D. *J Bone Miner Res.* 2005; 20(11):1944–1950. [PubMed: 16234967]
- Ding C, Buckingham B, Levine MA. Familial isolated hypoparathyroidism caused by a mutation in the gene for the transcription factor GCMB. *J Clin Invest.* 2001; 108(8):1215–1220. [PubMed: 11602629]
- Doyle D, Kirwin SM, Sol-Church K, Levine MA. A novel mutation in the GCM2 gene causing severe congenital isolated hypoparathyroidism. *J Pediatr Endocrinol Metab.* 2012; 25(7–8):741–746. [PubMed: 23155703]
- Fraser RA, Kronenberg HM, Pang PK, Harvey S. Parathyroid hormone messenger ribonucleic acid in the rat hypothalamus. *Endocrinology.* 1990; 127(5):2517–2522. [PubMed: 2226330]
- Germain-Lee EL, Schwindinger W, Crane JL, Zewdu R, Zweifel LS, Wand G, Huso DL, Saji M, Ringel MD, Levine MA. A mouse model of Albright hereditary osteodystrophy generated by targeted disruption of exon 1 of the *Gnas* gene. *Endocrinology.* 2005; 146(11):4697–4709. [PubMed: 16099856]
- Gordon J, Bennett AR, Blackburn CC, Manley NR. *Gcm2* and *Foxn1* mark early parathyroid- and thymus-specific domains in the developing third pharyngeal pouch. *Mech Dev.* 2001; 103(1–2):141–143. [PubMed: 11335122]
- Grigorieva IV, Mirczuk S, Gaynor KU, Nesbit MA, Grigorieva EF, Wei Q, Ali A, Fairclough RJ, Stacey JM, Stechman MJ, Mihai R, Kurek D, Fraser WD, Hough T, Condie BG, Manley N, Grosveld F, Thakker RV. *Gata3*-deficient mice develop parathyroid abnormalities due to dysregulation of the parathyroid-specific transcription factor *Gcm2*. *J Clin Invest.* 2010; 120(6):2144–2155. [PubMed: 20484821]
- Gunther T, Chen ZF, Kim J, Priemel M, Rueger JM, Amling M, Moseley JM, Martin TJ, Anderson DJ, Karsenty G. Genetic ablation of parathyroid glands reveals another source of parathyroid hormone. *Nature.* 2000; 406(6792):199–203. [PubMed: 10910362]
- Gupta A, Winer K, Econs MJ, Marx SJ, Collins MT. FGF-23 is elevated by chronic hyperphosphatemia. *J Clin Endocrinol Metab.* 2004; 89(9):4489–4492. [PubMed: 15356053]
- Hashemolhosseini S, Wegner M. Impacts of a new transcription factor family: mammalian GCM proteins in health and disease. *J Cell Biol.* 2004; 166(6):765–768. [PubMed: 15353544]
- Hitoshi S, Ishino Y, Kumar A, Jasmine S, Tanaka KF, Kondo T, Kato S, Hosoya T, Hotta Y, Ikenaka K. Mammalian *Gcm* genes induce *Hes5* expression by active DNA demethylation and induce neural stem cells. *Nat Neurosci.* 2011; 14(8):957–964. [PubMed: 21765423]
- Hosoya T, Takizawa K, Nitta K, Hotta Y. Glial cells missing: a binary switch between neuronal and glial determination in *Drosophila*. *Cell.* 1995; 82(6):1025–1036. [PubMed: 7553844]
- Jones BW, Fetter RD, Tear G, Goodman CS. Glial cells missing: a genetic switch that controls glial versus neuronal fate. *Cell.* 1995; 82(6):1013–1023. [PubMed: 7553843]
- Kamitani-Kawamoto A, Hamada M, Moriguchi T, Miyai M, Saji F, Hatamura I, Nishikawa K, Takayanagi H, Hitoshi S, Ikenaka K, Hosoya T, Hotta Y, Takahashi S, Kataoka K. MafB interacts

- with Gcm2 and regulates parathyroid hormone expression and parathyroid development. *J Bone Miner Res.* 2011; 26(10):2463–2472. [PubMed: 21713993]
- Kammerer M, Pirola B, Giglio S, Giangrande A. GCMB, a second human homolog of the fly glide/gcm gene. *Cytogenet Cell Genet.* 1999; 84(1–2):43–47. [PubMed: 10343099]
- Kim J, Jones BW, Zock C, Chen Z, Wang H, Goodman CS, Anderson DJ. Isolation and characterization of mammalian homologs of the *Drosophila* gene glial cells missing. *Proc Natl Acad Sci U S A.* 1998; 95:12364–12369. [PubMed: 9770492]
- Liu Z, Farley A, Chen L, Kirby BJ, Kovacs CS, Blackburn CC, Manley NR. Thymus-associated parathyroid hormone has two cellular origins with distinct endocrine and immunological functions. *PLoS Genet.* 2010; 6(12):e1001251. [PubMed: 21203493]
- Liu Z, Yu S, Manley NR. Gcm2 is required for the differentiation and survival of parathyroid precursor cells in the parathyroid/thymus primordia. *Dev Biol.* 2007; 305(1):333–346. [PubMed: 17382312]
- Mannstadt M, Bertrand G, Muresan M, Weryha G, Leheup B, Pulusani SR, Grandchamp B, Juppner H, Silve C. Dominant-Negative GCMB Mutations Cause an Autosomal Dominant Form of Hypoparathyroidism. *J Clin Endocrinol Metab.* 2008; 93(9):3568–3576. [PubMed: 18583467]
- Maret A, Bourdeau I, Ding C, Kadkol SS, Westra WH, Levine MA. Expression of GCMB by intrathymic parathyroid hormone-secreting adenomas indicates their parathyroid cell origin. *J Clin Endocrinol Metab.* 2004; 89(1):8–12. [PubMed: 14715818]
- Maret A, Ding C, Kornfield SL, Levine MA. Analysis of the GCM2 gene in isolated hypoparathyroidism: a molecular and biochemical study. *J Clin Endocrinol Metab.* 2008; 93(4):1426–1432. [PubMed: 18182452]
- Mirczuk SM, Bowl MR, Nesbit MA, Cranston T, Fratter C, Allgrove J, Brain C, Thakker RV. A missense glial cells missing homolog B (GCMB) mutation, Asn502His, causes autosomal dominant hypoparathyroidism. *J Clin Endocrinol Metab.* 2010; 95(7):3512–3516. [PubMed: 20463099]
- Nutley MT, Parimi SA, Harvey S. Sequence analysis of hypothalamic parathyroid hormone messenger ribonucleic acid. *Endocrinology.* 1995; 136(12):5600–5607. [PubMed: 7588314]
- O’Gorman S, Dagenais NA, Qian M, Marchuk Y. Protamine-Cre recombinase transgenes efficiently recombine target sequences in the male germ line of mice, but not in embryonic stem cells. *Proc Natl Acad Sci U S A.* 1997; 94(26):14602–14607. [PubMed: 9405659]
- O’Gorman S, Wahl GM. Mouse engineering. *Science.* 1997; 277(5329):1025. [PubMed: 9289845]
- Okabe M, Graham A. The origin of the parathyroid gland. *Proc Natl Acad Sci U S A.* 2004; 101(51):17716–17719. [PubMed: 15591343]
- Quinn SJ, Thomsen AR, Pang JL, Kantham L, Brauner-Osborne H, Pollak M, Goltzman D, Brown EM. Interactions between calcium and phosphorus in the regulation of the production of fibroblast growth factor 23 in vivo. *Am J Physiol Endocrinol Metab.* 2013; 304(3):E310–E320. [PubMed: 23233539]
- Schreiber J, Enderich J, Wegner M. Structural requirements for DNA binding of GCM proteins. *Nucleic Acids Research.* 1998; 26(10):2337–2343. [PubMed: 9580683]
- Silver J, Naveh-Many T. FGF23 and the parathyroid. *Adv Exp Med Biol.* 2012; 728:92–99. [PubMed: 22396164]
- Simmonds CS, Karsenty G, Karaplis AC, Kovacs CS. Parathyroid hormone regulates fetal-placental mineral homeostasis. *J Bone Miner Res.* 2010; 25(3):594–605. [PubMed: 19968565]
- Sticht H, Hashemolhosseini S. A common structural mechanism underlying GCMB mutations that cause hypoparathyroidism. *Med Hypotheses.* 2006; 67(3):482–487. [PubMed: 16697534]
- Thomee C, Schubert SW, Parma J, Le PQ, Hashemolhosseini S, Wegner M, Abramowicz MJ. GCMB mutation in familial isolated hypoparathyroidism with residual secretion of parathyroid hormone. *J Clin Endocrinol Metab.* 2005; 90(5):2487–2492. [PubMed: 15728199]
- Wegner M, Riethmacher D. Chronicles of a switch hunt: gcm genes in development. *Trends Genet.* 2001; 17(5):286–290. [PubMed: 11335039]
- Yamashita H, Yamazaki Y, Hasegawa H, Yamashita T, Fukumoto S, Shigematsu T, Kazama JJ, Fukagawa M, Noguchi S. Fibroblast growth factor-23 (FGF23) in patients with transient

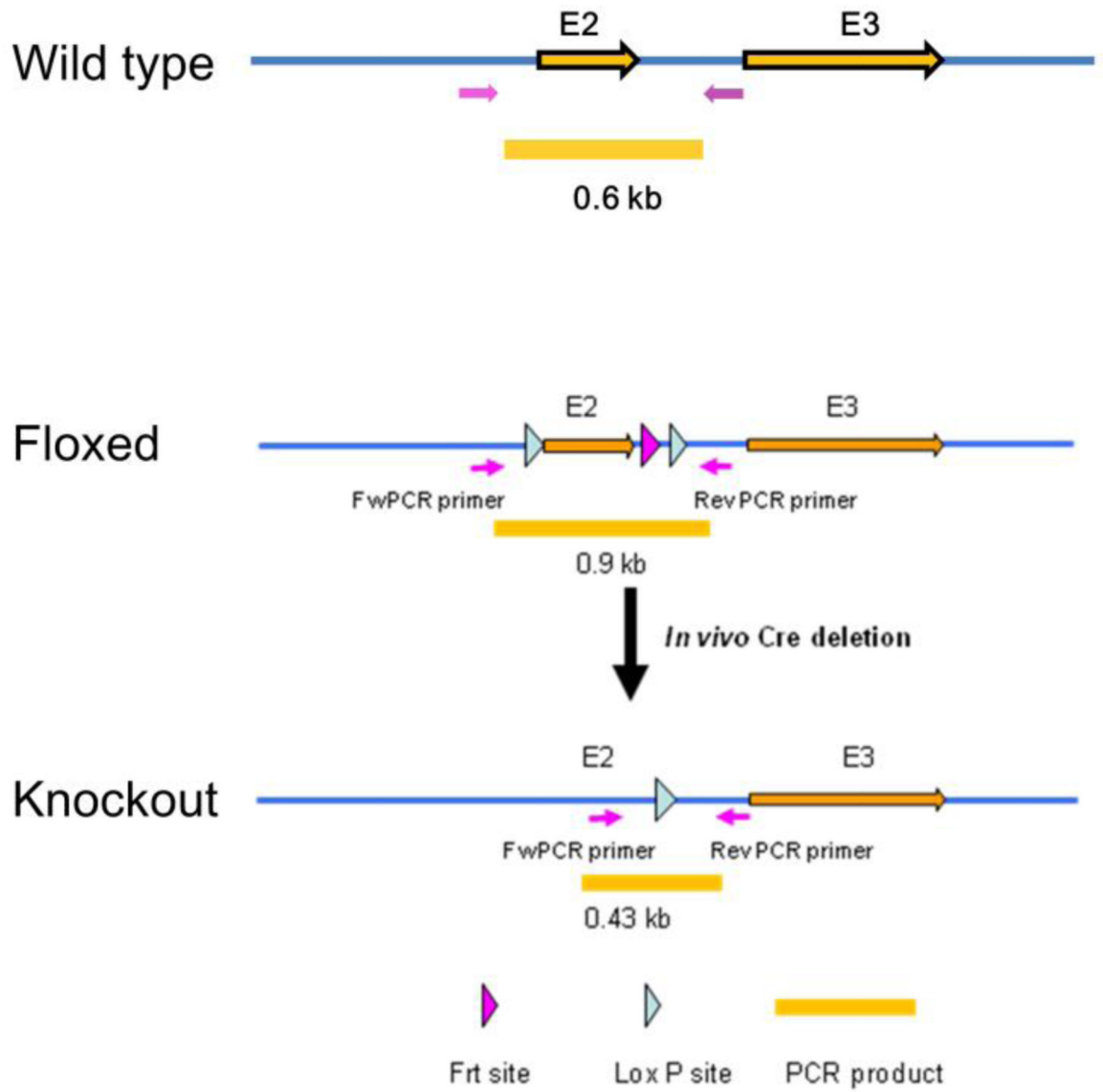
hypoparathyroidism: its important role in serum phosphate regulation. *Endocr J.* 2007; 54(3):465–470. [PubMed: 17464094]

Yuan Q, Jiang Y, Zhao X, Sato T, Densmore M, Schuler C, Erben RG, McKee MD, Lanske B. Increased osteopontin contributes to inhibition of bone mineralization in FGF23-deficient mice. *Journal of bone and mineral research : the official journal of the American Society for Bone and Mineral Research.* 2013

Zajac JD, Danks JA. The development of the parathyroid gland: from fish to human. *Curr Opin Nephrol Hypertens.* 2008; 17(4):353–356. [PubMed: 18660669]



E.



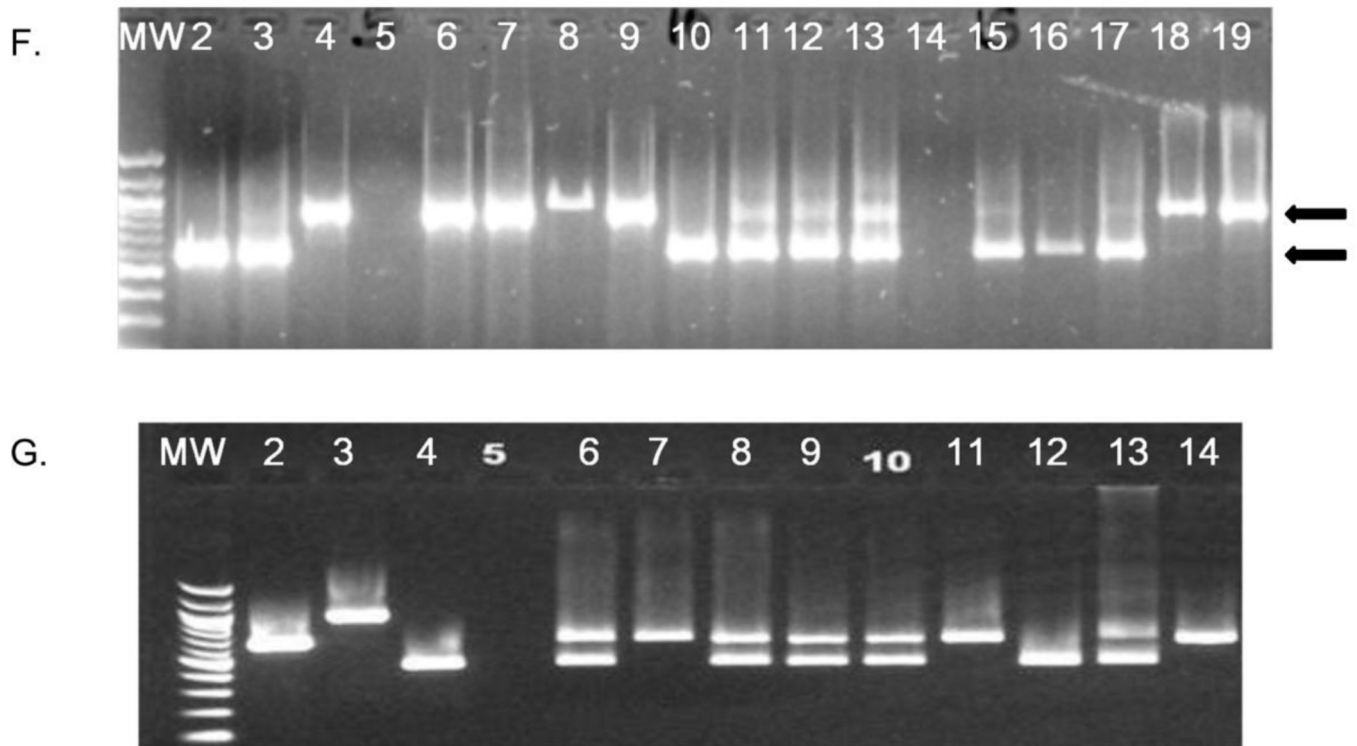


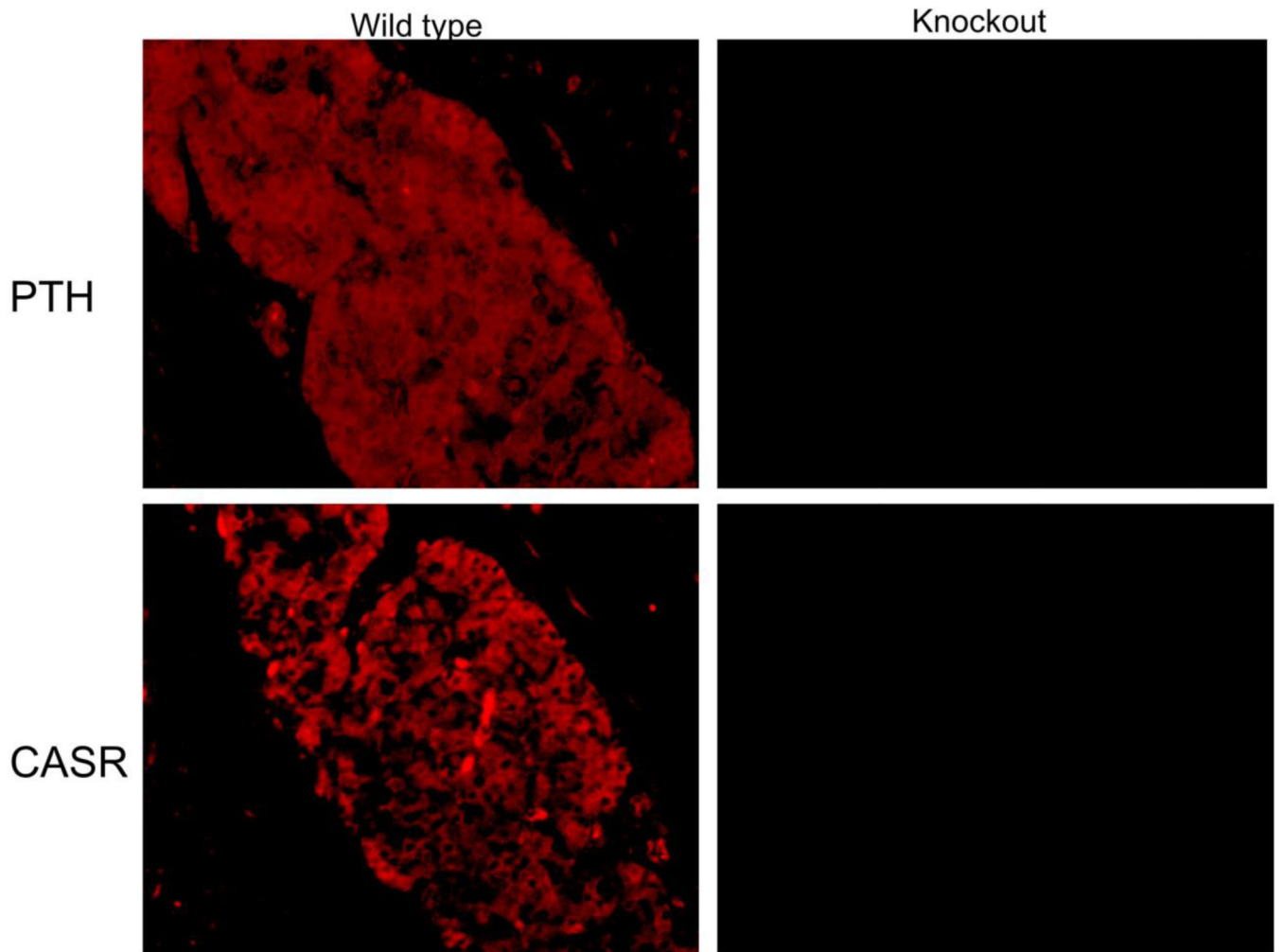
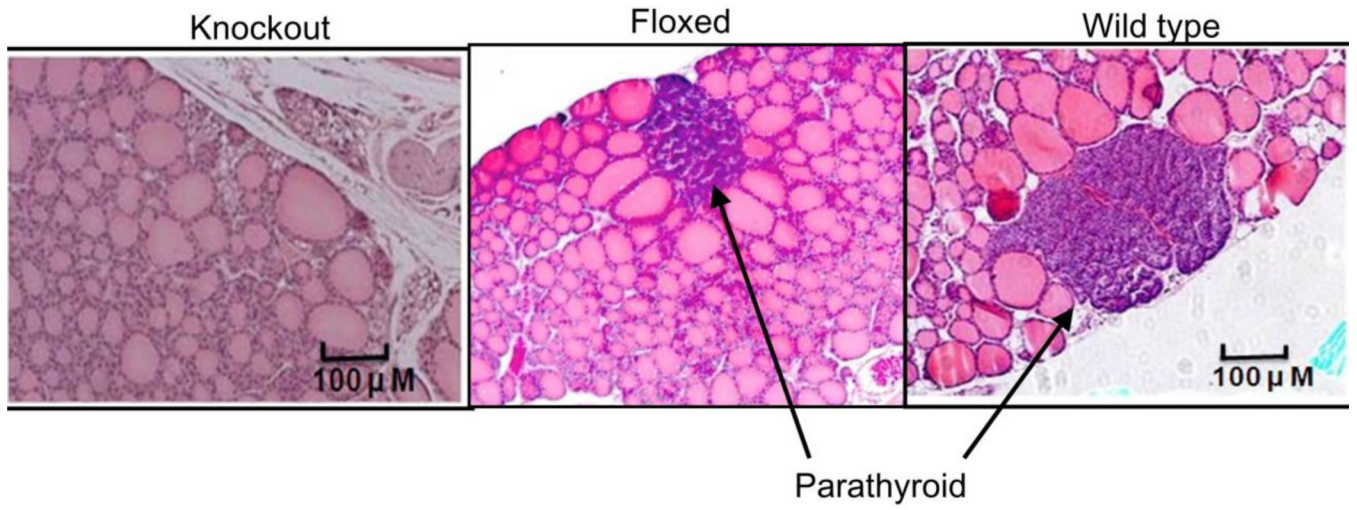


Figure 1. Targeting vector strategy

A. the mouse *Gcm2* gene is located on chromosome 13 and is organized into five exons, with exon 1 containing the start codon and the first 30 amino acids of the protein, exon 2 (E2) containing the entire GCM motif, and exons 3–5 encoding the C-terminal two thirds of the protein. **B.** the initial targeting vector (*LoxFTNwCD/mGcm2*) was approximately 14.2 kb, and contained a 5' arm of homology (approximately 4.2 kb), a 3' arm of homology (approximately 4.0 kb) and a *neo^r* cassette for positive selection that was flanked by FRT sites. Exon 2 (E2) is flanked by *loxP* sites. A DTA cassette encoding diphtheria toxin for negative selection was placed after the 3' arm. **C.** the upper panel shows the targeting construct that was electroporated into B6-3 ES (C57BL/6) cells with selection by G418. The positions of the three hybridization probes are noted. **D.** Southern blot of genomic DNA from four G418-resistant clones (C5, E8, H3 and H11) that were identified by primary screening by PCR and B63, a negative control. Restriction analysis of DNA from clones H11 and E8 generated hybridizing fragments of the predicted sizes (arrows) with all three probes, thus confirming proper homologous recombination. **E.** Schematic of the wild type (upper) and floxed (middle) *Gcm2* allele and the final *Gcm2* allele (lower) after excision of the exon 2 region by Cre recombinase. Diagram shows sizes of PCR products and positions of primers used for genotyping by PCR. **F.** Panel shows PCR genotyping using genomic DNA from F1 offspring of both E8 and H11 chimera mice. The conditional knockout allele is predicted to generate a 0.9 kb fragment (upper arrow) and the wild type allele is predicted to generate a 0.6 kb fragment (lower arrow). Lane MW, 100 bp ladder; lane 5 is water control template and lane 14 is intentionally blank. Mice that are wild type, heterozygous and homozygous for the conditional allele can be readily distinguished. **G.** Panel shows PCR genotyping using genomic DNA from offspring of matings between E8 founder mice and

Prm-Cre mice. The conditional knockout allele ($Gcm2^{E2fl}$) is predicted to generate a 0.9 kb fragment (lane 3) and the wild type allele is predicted to generate a 0.6 kb fragment (lane 2), and the recombined allele ($Gcm2^{-E2}$) is predicted to generate a 0.4 kb fragment (lane 4). Lane MW, 100 bp ladder and lane 5 is a water control template. Mice that are heterozygous (lanes 6, 8, 9, 10 and 13) or homozygous (lane 12) for the exon 2-deleted *Gcm2* allele are readily distinguished from wild type mice (lanes 7, 11 and 14).  Denotes loxP site and  denotes Frt site.



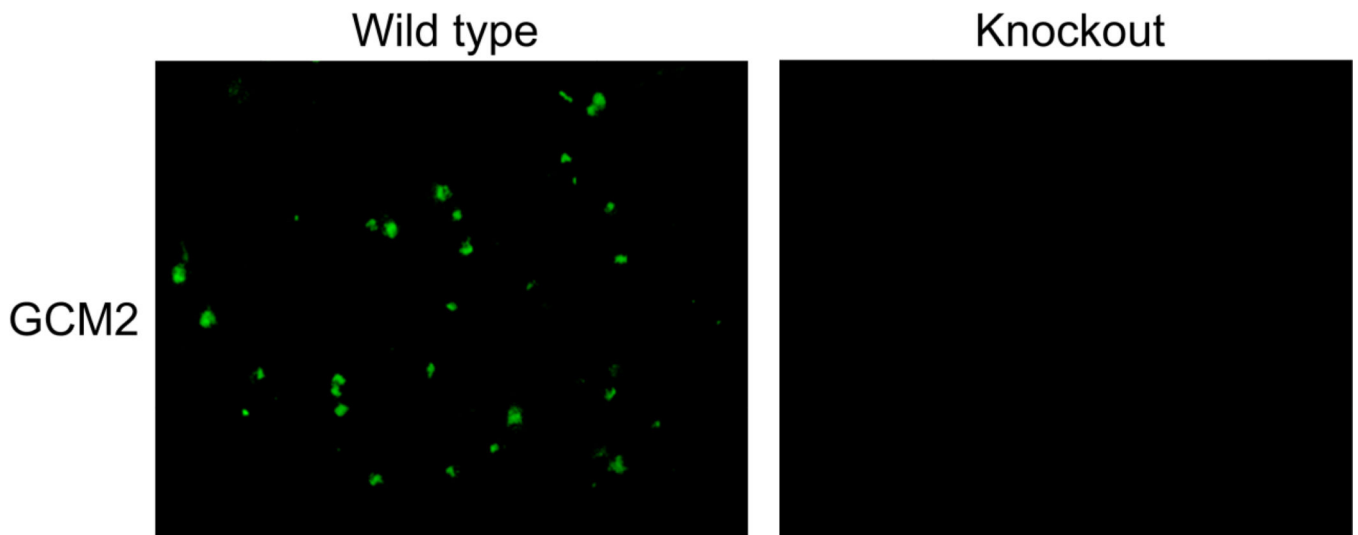


Figure 2. Parathyroid and neck anatomy

A. Histological analysis of tracheal sections from 30-day wild type, floxed, and knockout mice. Panels show H&E staining and 2.5× magnification. No parathyroid tissue is present in the neck of knockout mice. **B.** Immunofluorescence analysis of the expression of PTH and CASR (red) in wild type and knockout mice. **C.** Immunofluorescence analysis of the expression of GCM2 (green) in wild type and knockout mice.

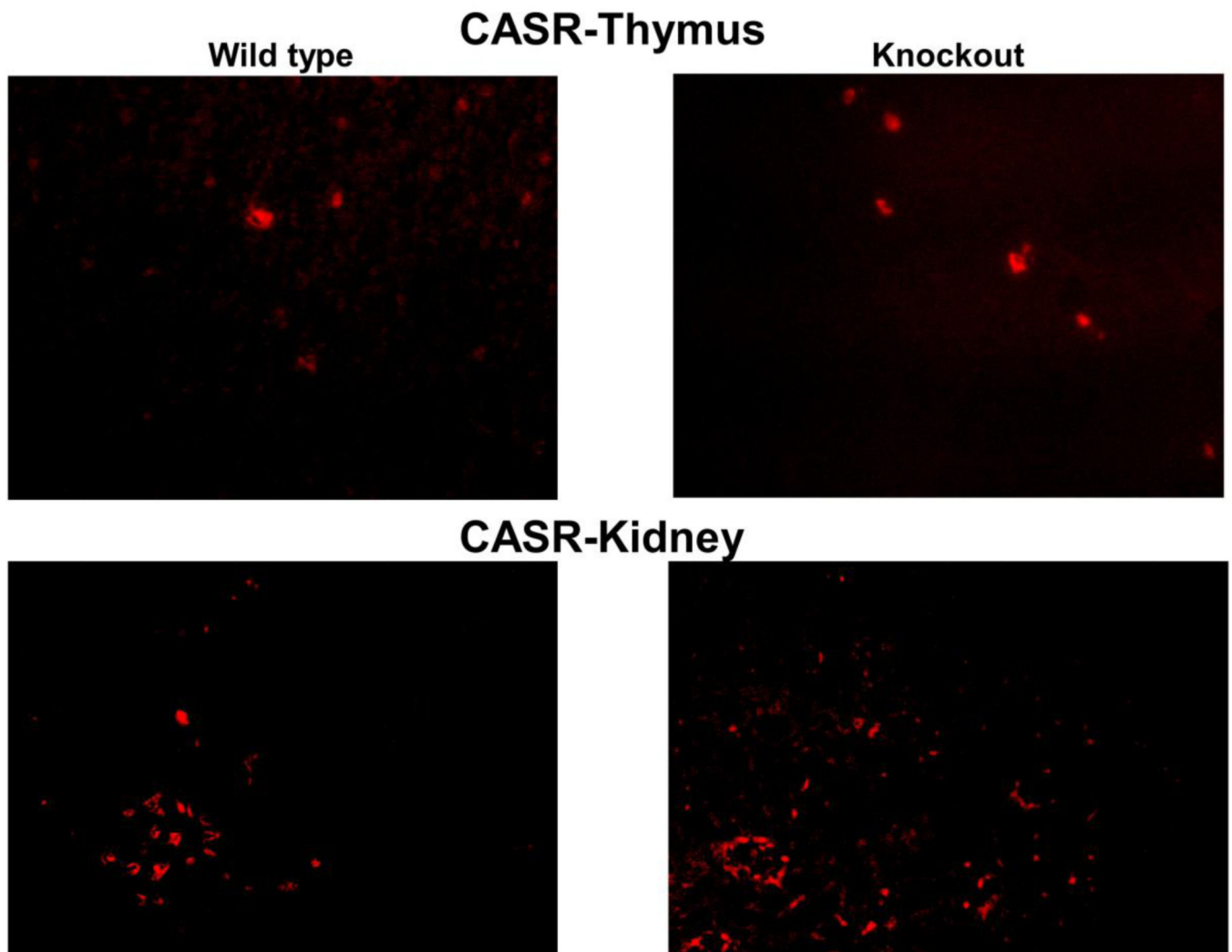


Figure 3. Expression of CASR in thymus and kidney

Genotype of mice is noted above each panel. Immunofluorescence (IF) analysis of the expression of CASR in thymus and kidney tissues from wild type (left) and knockout (right) mice at 30 days of age. CASR was stained red with anti-CASR Ab (Alexa Fluoro 647).

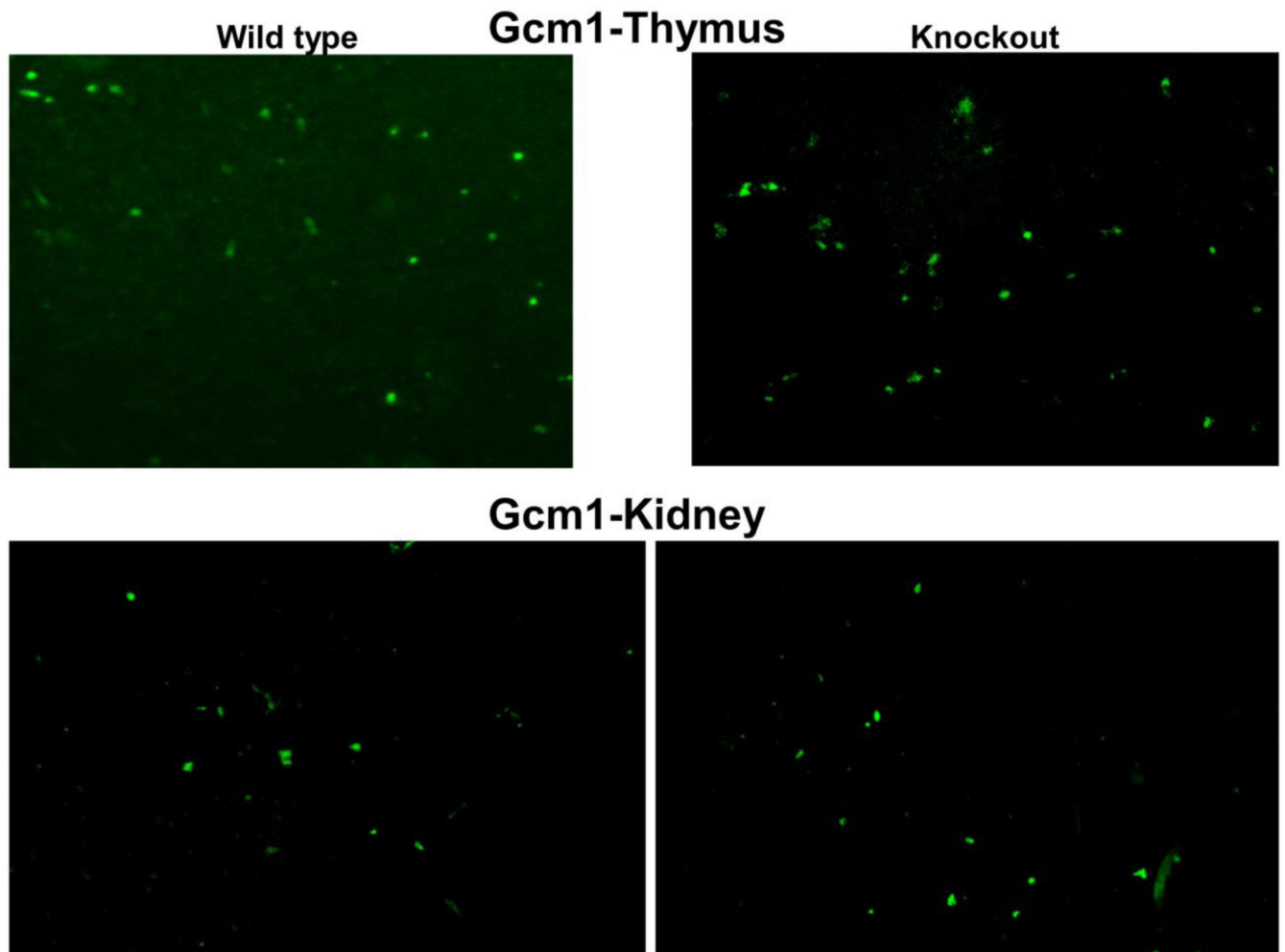


Figure 4. Expression of GCM1 in thymus and kidney

Genotype of mice is noted above each panel. Immunofluorescence (IF) analysis of the expression of GCM1 in thymus and kidney tissues from wild type (left) and knockout (right) mice at 30 days of age. GCM1 was stained green with anti-GCM1 Ab (Alexa Fluoro 488).

Table 1

Physical and biochemical measurements from mice at 6 months of age.

	Wild type	Floxed	Knockout
Number	22	9	23
Weight, gram	36.6 ± 7	36.2 ± 6	35.3 ± 7.1
Length, cm	3.7 ± 0.1	3.7 ± 0.2	3.6 ± 0.2
sCalcium, mg/dL	9.9 ± 1.0	10.3 ± 0.9	7.0 ± 1.5*
sPhosphorus, mg/dL	6.1 ± 1.0	6.8 ± 0.6	9.6 ± 2.1*
PTH intact, pg/mL	158.7 ± 177	156.3 ± 50.4	32 ± 27*

Data are ± SD.

* p <0.001 versus wild type.